

Article

Tensile Properties of Aluminum Matrix Composites Produced via a Nitrogen-Induced Self-Forming Process

Kon-Bae Lee ^{1,*}, Kanhu C. Nayak ¹, Cheol-Hwee Shim ², Hye-In Lee ³, Se-Hoon Kim ³, Hyun-Joo Choi ^{1,*} and Jae-Pyoung Ahn ^{4,*}

¹ Department of Materials Science and Engineering, Kookmin University, Seoul 02707, Republic of Korea; nayakkanhu83@gmail.com

² Advanced Analysis Center, Korea Institute of Science and Technology (KIST), Seoul 02792, Republic of Korea

³ Advanced Materials R&D Department, Korea Automotive Technology Institute (KATECH), Cheonan-si 31214, Republic of Korea; hilee@katech.re.kr (H.-I.L.); shkim@katech.re.kr (S.-H.K.)

⁴ Advanced Analysis and Data Center, Korea Institute of Science and Technology (KIST), Seoul 02792, Republic of Korea

* Correspondence: kblee@kookmin.ac.kr (K.-B.L.); hyunjoo@kookmin.ac.kr (H.-J.C.); jpahn@kist.re.kr (J.-P.A.); Tel.: +82-10-8533-9875 (H.-J.C.)

Abstract: This study compares the tensile properties of commercial aluminum matrix composites (AMCs) with those of AMCs produced via a nitrogen-induced self-forming process. This process is a newly developed AMCs manufacturing process that takes advantage of the price competitiveness and productivity of large-scale products produced via the liquid process. Additionally, this process has the freedom of choice of the reinforcement phase and the homogeneous dispersibility of the powder process. Compared to commercial monolithic 6061 alloys, 6061 aluminum alloy matrix composites exhibit increased Young's modulus, yield strength, and ultimate tensile strength by 59%, 66%, and 81%, respectively. This study also compares the tensile properties of AMCs with different matrix compositions, including 2009 and 7050 aluminum alloys. The study shows that AMCs produced using the nitride-induced self-forming aluminum composite (NISFAC) process exhibit comparable or superior tensile properties to those obtained using existing commercial powder metallurgy (P/M) processes.

Keywords: aluminum matrix composite; interface bonding; microstructure; nitridation; tensile strength



Citation: Lee, K.-B.; Nayak, K.C.; Shim, C.-H.; Lee, H.-I.; Kim, S.-H.; Choi, H.-J.; Ahn, J.-P. Tensile Properties of Aluminum Matrix Composites Produced via a Nitrogen-Induced Self-Forming Process. *J. Compos. Sci.* **2023**, *7*, 457. <https://doi.org/10.3390/jcs7110457>

Academic Editors: Oscar Marcelo Suárez and Hongseok Choi

Received: 25 September 2023

Revised: 23 October 2023

Accepted: 30 October 2023

Published: 2 November 2023



Copyright: © 2023 by the authors. Licensee MDPI, Basel, Switzerland. This article is an open access article distributed under the terms and conditions of the Creative Commons Attribution (CC BY) license (<https://creativecommons.org/licenses/by/4.0/>).

1. Introduction

Metal matrix composites (MMCs) are tailored with desired properties by adding ceramic reinforcing phases to a metal matrix, which can be controlled via the type, shape, volume fraction, and distribution. Aluminum metal matrix composites (AMCs) have excellent mechanical and thermal properties, making them highly value-added to the automobile, electronics, and aerospace industries [1–5]. Therefore, the MMCs market continues to grow at an annual growth rate of about 6.3% and the total market size is expected to exceed 433.3 million USD in 2022 [6]. In particular, AMCs are the largest product segment, accounting for more than 30% of the total MMCs market. The continuous AMCs market expansion is expected due to the high demand for high-specific-strength materials required in the automobile and aerospace industries [5,7].

The application of AMCs can be broadly classified into two categories: one is a structural application and the other is thermal management. AMCs have superior specific strength and specific stiffness compared to lightweight metal alloys (e.g., Al, Mg) [8–11] and also have excellent price competitiveness compared to carbon fiber reinforcement polymer (CFRP) and glass fiber reinforcement polymer (GFRP). Tran et al. [12,13] investigated the tensile strength and stiffness aligned in the fiber direction of CF and CNT reinforcement composite wire using the Cu matrix. Remarkably, considering most of the structural

materials are subjected to load in a multiaxial direction, AMCs are advantageous in that they have 3D isotropy due to discontinuous reinforcement dispersed in the Al matrix compared to CFRP or GFRP, which shows good properties only along the longitudinal axis of the fiber. The anisotropy effect on the mechanical properties of glass and carbon fiber polymer composites was explored by researchers, where tensile strength is greater in the direction of fiber alignment [14–16]. In addition, AMCs show excellent environmental resistance (chemicals, organic fluids, and radiation), wear and abrasion resistance, impact toughness, and fatigue resistance compared to the polymer matrix composite; thus, they are used in automobile pistons, engines, cylinders, etc. [3,9,17–20]. It is expected that the application in the field of structural materials will continue to expand. However, to secure a stable market for AMCs, which occupy an intermediate position between alloys and polymer composites in terms of mechanical and price competitiveness, continuous efforts are needed for properties and price competitiveness that exceed those of competitive materials.

AMCs with high thermal conductivity (TC) and low coefficient of thermal expansion (CTE) [21–23], which have excellent compatibility with semiconductor materials and can quickly dissipate heat, are gradually expanding in various fields such as computer chips, power devices [24], and electronic packaging [25,26]. However, AMCs are challenging to control the coefficient of thermal expansion compared to Kovar or Invar and have lower thermal conductivity than pure metals (e.g., Al, Cu), so securing a market that can replace competitive materials is difficult. Therefore, by taking the unique advantage of composite materials that can tailor the exact target properties according to the type, geometry, and volume of the reinforcement phase or by realizing the range of properties that cannot be achieved by single materials, which are competitive in the thermal management field, it is necessary to establish a market that can guarantee a solid superiority over competitive materials.

As discussed above, composite materials generally have an ambiguous position between conventional materials (light alloys) and cutting-edge (high-tech) materials regarding price competitiveness and physical properties, so they are constantly being threatened by competitive materials to secure their market share. Therefore, for the continuous market expansion of AMCs, it is essential to develop a competitive new manufacturing process with the flexibility of selection of the reinforcement type, geometry, and volume, while maintaining the unique advantages of composite materials.

A commercial AMCs manufacturing technique can be divided into a liquid-state process and a solid-state process, as summarized in Figure 1. Liquid-state processes include stir casting [27,28] and infiltration [29], while solid-state processes generally use powder metallurgy (P/M) [30]. Stir casting is of low cost but has limitations in dispersing and controlling reinforcement particles. Infiltration is widely used for thermal management but has limitations in manufacturing and unwanted second phases. The P/M process allows for any shape and size of the reinforcement phase and has the advantage of excellent physical properties. However, this process involves multiple process steps to manufacture the final product, as shown in Figure 1, and therefore, the manufacturing process cost is high compared to other methods. However, the intermediate manufacturing steps are not crucial for the self-sintering-based technique compared to other processes, as shown in Figure 1. Table 1 summarizes the advantages and disadvantages of each process [31]. Recently, via continuous research for process improvement, we developed a new concept of AMCs manufacturing process based on self-sintering that breaks the conventional notion that overcoming (or improving) the wettability between Al and ceramic-reinforced phases is essential in manufacturing AMCs. This self-sintering-based manufacturing method is called the Nitride-induced Self-Forming Aluminum Composite (NISFAC) process. The NISFAC process is an innovative and simple process that can simultaneously take advantage of the price competitiveness and productivity of large-scale products of the liquid process, as well as the freedom of choice of the reinforcement phase and the homogeneous dispersibility of the P/M process. Specifically, the NISFAC process involves mixing raw materials (Al powder and desired reinforcement), heating in a nitrogen atmosphere, and secondary

processing (optional). Not only is the number of processes reduced compared to the existing process (Figure 1), but each process is straightforward without needing special equipment and the know-how (Table 1).

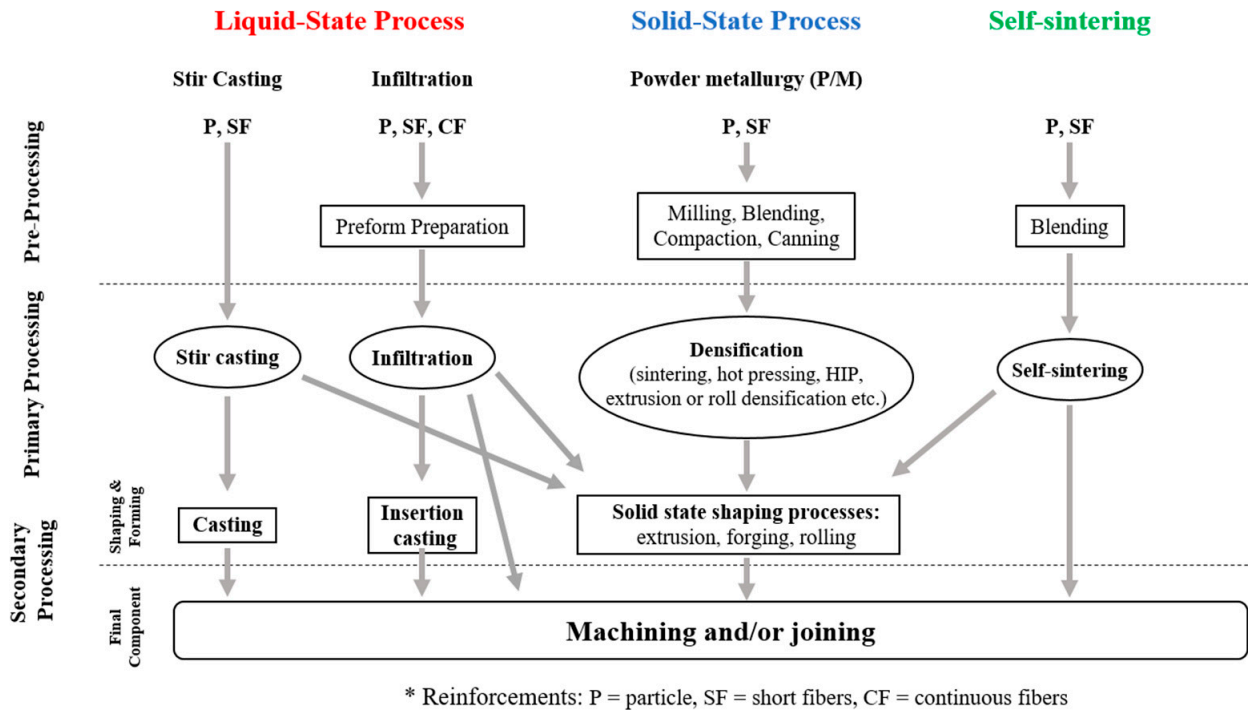


Figure 1. Comparison of MMCs manufacturing techniques [27] (permission taken from Elsevier).

Table 1. Comparison of commercial AMC techniques with the NISFAC method [31].

	Stir Casting	Infiltration	Powder Metallurgy	NISFAC Process
Advantages	<ul style="list-style-type: none"> Low cost Enable us to produce large-scale products 	<ul style="list-style-type: none"> Low/medium cost 	<ul style="list-style-type: none"> Flexible in materials design Low processing temperatures 	<ul style="list-style-type: none"> Low processing temperature and limited unfavorable reaction, flexibilities in materials design Near-net shape forming Mg-free, pressure-free process, cost-effective
Disadvantages	<ul style="list-style-type: none"> Low quality High processing temperature (unfavorable reactants) Poor wetting between reinforcement and the matrix 	<ul style="list-style-type: none"> Requires preforms, additives, and pressure Poor wetting between reinforcement and the matrix 	<ul style="list-style-type: none"> High process cost Complex process Difficulties in near-net shape forming 	<ul style="list-style-type: none"> A limited range of matrix material selection that involves exothermic reaction with a sufficient heat release
Remarks	<ul style="list-style-type: none"> Suitable for discontinuous fibers, especially particulate reinforcement Widely used in automotive, aerospace, industrial equipment, and sporting industries, used to manufacture bearing materials 	<ul style="list-style-type: none"> Strong anisotropy Used to produce structural shapes such as rods, tubes, and beams with maximum properties in a uniaxial direction 	<ul style="list-style-type: none"> Mainly used to produce small objects (especially round bolts, pistons, valves, high-strength, and heat-resistant materials) 	<ul style="list-style-type: none"> A variety of combinations of material types, sizes, shapes, and composition No requirement for additional equipment (or processes) so it can extend the scope of potential applications

Previous studies reported the mechanisms and process parameters by which AMCs are manufactured [32–34]. In other words, it was explained that the new process has sufficient competitiveness compared to the existing commercial process. In that direction, a further investigation of the characteristics of the AMCs manufactured via the novel process (e.g., NISFAC) is essential. Therefore, in this study, the level of tensile properties of AMCs

manufactured via the new NISFAC process was compared to those of the P/M method, which are commonly evaluated as having superior mechanical properties compared to other processes. In addition, the behavior of tensile strength of AMCs and their matrix–reinforcement interfaces were examined via the microstructure.

2. Experimental

AMCs were synthesized using the NISFAC process followed by hot extrusion in the present work. As mentioned, the NISFAC process consists of three steps: powder mixing, heating, and secondary processing (optional). First, SiC particles (average particle size: ~9.7 μm, purchased from Showa Denko, Minato-ku, Tokyo, Japan) were added to various aluminum alloy powders (average powder size: ~7–10 μm, purchased from Chengdu Best New Materials Co., Ltd., Pitong Town, Chengdu, China), namely AA2009, 6061, and 7050. The volume fraction of SiC particles was 15–25%. The Al and SiC particles were mixed using a turbula mixer (DM-T2, Daemyoung Enterprise Co., Ltd., Dobong-gu, Seoul, Republic of Korea) without milling media (e.g., balls) or a process control agent. The mixed powder was placed in a graphite crucible and lightly tapped, charged into a furnace, and heated for 1.5 to 2 h at 650 to 670 °C under a nitrogen atmosphere. After that, it was removed from the furnace and air-cooled. The heating rate was 5 °C/min, while the nitrogen flow rate was 3 L/min. The prepared AMCs were extruded at 350 °C at an extrusion ratio of 18:1 to produce an extruded rod with a final diameter of 16 mm. After extrusion, the NISFAC-based AMCs containing 6061, 6063, 7050, and 2009 in this study are designated as 6061/PS, 6063/PS, 7050/PS, and 2009/PS, respectively (here, PS stands for the present study). Similarly, the designation of other commercial composites developed via various companies is presented in Table 2.

Table 2. Summary of mechanical properties of different composites and their matrix (PS: present study; ER: extrusion ratio; Nr: degree of nitridation; E: Young’s modulus; UTS: ultimate tensile strength; YS: yield stress; el.: elongation) [35,36].

Matrix Alloys	AMCs	SiC Size (μm)	SiC Vol.%	Matrix Size (μm)	Density (gcm ³)	E _y (GPa)	YS (MPa)	UTS (MPa)	el. (%)	ER	Nr (%)
6061 (T6)	6061 Al	---	---	---	2.7	68.9	276	310	12	---	---
	6061/PS	9.7	17.5	10	2.789	110 (±2.5)	457 (±10.62)	560 (±4.78)	4.5 (±0.23)	18:1	1.9
	6061/Materion	2–3	40	---	2.9	140	490	620	2.5	---	---
6063 (T6)	6063 Al	---	---	---	2.7	68.9	214	241	12	---	---
	6063/PS	14.5	17.5	74	2.8	105 (±3.1)	306 (±8.6)	381 (±10.5)	10 (±1.75)	18:1	0.5
6092 (T6)	6092 Al	---	---	---	2.7	73.8	290	366	---	60:1	---
	6092/DWA	---	17.5	---	2.79	106	421	490	6	60:1	---
7050 (T6)	7050 Al	---	---	---	2.83	71.7	490	552	11	---	---
	7050/PS	9.7	15	10	2.92	103 (±2.7)	487 (±6.5)	606 (±7.7)	4.7 (±0.76)	18:1	1.7
	7050/DWA	9.48	15	~45	---	98.7	506	538	1.2	14:1	---
2009 (T4)	2009 Al	---	---	---	2.7	69	324	469	19	---	---
	2009/PS	9.7	17.5	10	2.87	93 (±2.8)	444 (±7.5)	570 (±6.28)	4.4 (±1.1)	18:1	1.9
	2009/DWA	---	15	---	2.84	96	379	572	8.5	---	---
2124 (T4)	2024/Materion	2–3	25	---	2.88	115	480	680	5	---	---

The microstructures were observed using an optical microscope (OM, Eclipse LV100ND, Nikon, Minato-ku, Tokyo, Japan). The cross-sectional samples for OM were cut from the extruded bar. First, the samples were polished using 400-, 600-, 800-, and 1200-grade sandpapers. After that, final polishing was performed using the 0.3 μm alumina suspension for 20 mins and then cleaned with ethanol via a sonicator. Finally, optical images were taken using an optical microscope. The tensile test specimens were prepared using the ASTM E8 standard of a 25 mm gauge length, a 6 mm gauge width, and a 1 mm thickness. The tensile test was repeated 3 to 5 times for each specimen at an initial strain rate of 10⁻⁴/s

at room temperature of 25 °C (Instron 5967, Instron, Norwood, MA, USA) to evaluate the mechanical properties of AMCs. After the tensile test, the fracture surfaces of the specimens were observed using a scanning electron microscope (SEM, JEOL, JSM 2001F, Akishima, Japan). Samples were prepared using focused ion beam milling (FIB, Quanta 3D, FEI Co., Ltd., Hillsboro, OR, USA) and then transmission electron microscopy (TEM) (Titan 80-300, FEI Co., Hillsboro, OR, USA) to observe the interfacial structure between the Al and SiC particles.

3. Results and Discussion

3.1. Tensile Properties

Figure 2 illustrates the comparison of the tensile properties of monolithic 6XXX alloys (Al6061, Al6063, and Al6092) and 6XXX alloy matrix (Al6061, Al6063, and Al2009) composites, which were produced in this study and by representative commercial P/M companies, such as DWA (DWA, Aluminum Composites, Chatsworth, CA, USA) [35] and Materion products [36]. Density, yield strength, ultimate tensile strength, and elongation to failure of the AMCs produced in the present study are also summarized in Table 2. The representative stress–strain curves of all composites (6061/PS, 6063/PS, 7050/PS, and 2009/PS) are presented in Figure A1 in Appendix A. While there are variations in the material features (e.g., the size and volume fraction of SiC particles and the composition of the matrix) and processing parameters (e.g., extrusion temperature and ratio), it is still possible to relatively compare the performance of those specimens. In the case of the 6061 Al matrix, Young's modulus (E), yield strength (YS), and ultimate tensile strength (UTS) of our AMCs containing 17.5 vol.% SiC (~9.7 μm) were increased by 59%, 66%, and 81%, respectively, compared to commercial monolithic 6061 alloys. Similarly, E, YS, and UTS of the 6063/PS composite increased by 52, 43, and 58%, respectively, compared to their matrix Al (Figure 2). It can be noticed that (Figure 2), the 6061/17.5 vol% SiC composite (6061/PS) in the present study has higher tensile properties than other 6XXX Al (e.g., 6063 and 6092) matrix commercial composites containing SiC; this may be due to the smaller SiC particle size in the present study. On the other hand, the tensile properties of all the composites produced by Materion (AMC640XA) are superior compared to those produced in the present study, possibly due to the very fine sizes (2~3 μm) and high volume fraction (25–40%) of SiC particles in Materion's composites. Due to its outstanding mechanical properties, AMC640XA has various potential applications, including precision and high-speed machinery, aerospace, defense, and the automotive sector. Considering that the SiC particle size and volume fraction have a significant effect on the tensile properties of AMCs, it can be seen that our products have excellent tensile properties. Although there is no direct comparison of tensile data, it can be seen that the tensile properties of the 6063 Al matrix composite manufactured via the NISFAC process are comparable to those of commercial AMCs by DWA's 6092 Al matrix composite and 6063 Al alloys (Figure 2). Concerning the SiC vol.% of ~15% and the SiC size of ~9.7 μm, 7050/PS shows ~4% and ~13% higher Young's modulus and tensile strength, respectively, compared to 7050/DWA (Table 2). Similarly, the yield strength of 2009/PS is ~1.2 times that of 2009/DWA. In particular, DWA's products have an extrusion ratio of 60:1, which is higher than ours. This product is suggested as a suitable material for aviation structures and was used for the ventral fins and fuel access covers of F-16 Falcon fighters.

The tensile properties for composites of 2009 and 7050 Al matrices are shown in Figure 3. Alloy 7050 Al was treated with T6, and in the case of 2009 Al, the tensile properties of 2024 Al with a similar composition under the T4 condition were used as a standard. The mechanical properties such as E and UTS of the 7050/PS composite increased by 44 and 10%, respectively, compared to their matrix Al (Figure 3) except YS. Similarly, E, YS, and UTS of the 6063/PS composite increased by 35, 37, and 22%, respectively, compared to their matrix Al (Figure 3). In the case of commercial 7050 Al, which has very high strength, it has similar characteristics to that of DWA [35], although the effect of adding reinforcement is relatively smaller compared to 6XXX Al. In the case

of the 7050 Al composite, the SiC particle size (~9.5 μm), volume fraction (15%), and extrusion ratio (14:1) of both our and DWA were under similar conditions. In addition, the 7050 Al/SiC composite manufactured via the NIAFAC process shows slightly higher mechanical characteristics than DWA. However, when the matrix composition was 2XXX Al, the tensile properties were significantly improved by adding the reinforcing phase to their matrix alloy. Materion composite (AMC225XE) has a SiC particle size of 2–3 μm and a volume fraction of 25% and shows higher values of tensile properties than other materials, as seen in Figure 3 [36]. As mentioned previously, it can be due to the finer SiC particles and higher volume fraction in the 2124 Al matrix.

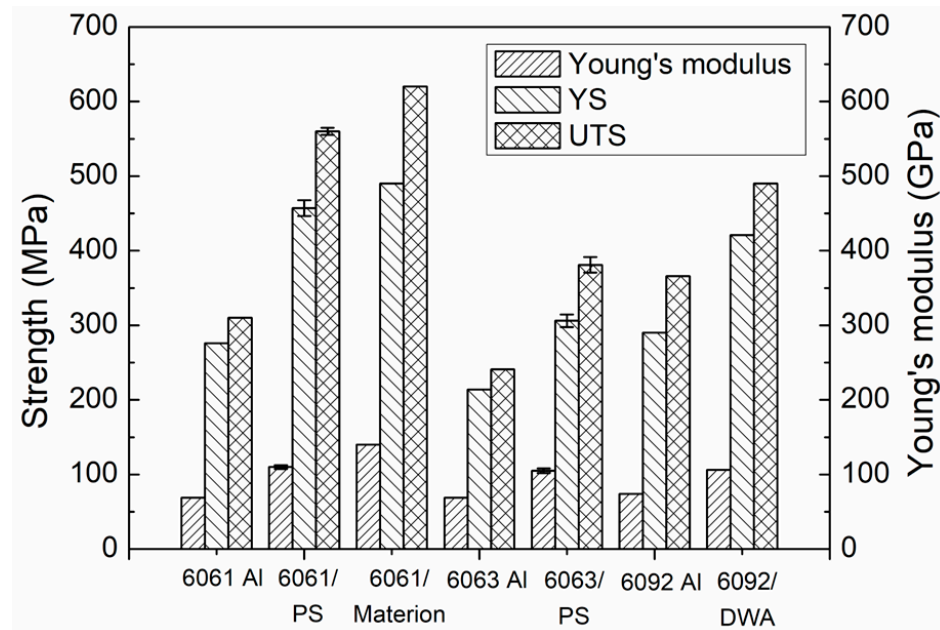


Figure 2. Mechanical properties of NISFAC-based Al6061/SiC and Al6063/SiC composite compared with commercial composite and their matrix.

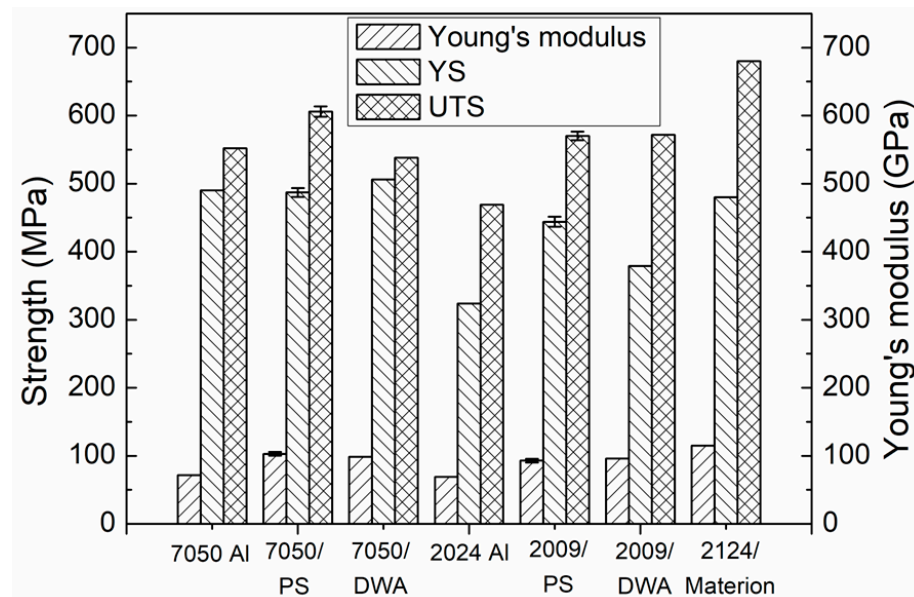


Figure 3. Mechanical properties of NISFAC-based Al7050/SiC and Al2009/SiC composite compared with commercial composite and their matrix.

In addition to the strength, the true stress–logarithmic strain curve of AMCs composites manufactured via the NISFAC process has been modeled with power law to examine

the flow stress behavior via a strain hardening exponent. An attempt has been made to compare the work-hardening exponent n regarding the power law represented by $\sigma = K\varepsilon^n$, wherein σ is the flow stress and K is constant. The flow curves of developed AMCs are presented in Figure A2 in Appendix A. A positive n value implies that flow strain hardening is the dominant mechanism for strain rates between 10^{-2} to 10^{-5} /s [37] (here, it is 10^{-4} /s). The magnitude of n is relatively higher than their matrix. The work hardening exponent of the Al 6061 heat-treated alloy is ~ 0.05 – 0.07 [38,39], while the Al6061/SiC composite in this study shows ~ 0.13 and is the highest for the 2009/SiC composite (~ 0.15). The higher value of n is caused by a higher dislocation storage capacity by the existence of SiC in the Al matrix, which impedes the movement of dislocation, and dislocations are accumulated near the Al–SiC interface, resulting in the improvement of mechanical properties in the present AMCs. In another way, the AMCs with higher values of n have a higher straining effect (resistance to thinning) against the plastic deformation while making the products.

From the results presented in Table 2, the tensile properties of the composite manufactured via the NISFAC process are similar to or superior to those obtained in the existing commercial P/M process. Moreover, it is essential that these mechanical properties were obtained from a composite manufactured via a process that is incomparably simpler than the P/M process. In other words, the NISFAC process proves it is a process that is capable of manufacturing AMCs with characteristics equal to or superior to those of existing commercial AMCs as well as their price.

3.2. Microstructural Features

Figure 4 shows the distribution of SiC particles (Figure 4a–c) and the fracture surface after the tensile tests (Figure 4d–f) in the composites with different matrices. It has been observed that the SiC particles are not only relatively uniformly distributed on the Al matrix but also form intimate contact with the matrix (Figure 4a–c). In addition, it was found that ductile failure of the Al matrix with dimples occurred in all composites regardless of the Al matrix composition, as shown in Figure 4d–f. The fracturing of SiC particles was observed instead of a pulled-out impression on the matrix. The breakage of SiC particles instead of de-cohesion at the Al–SiC interface suggests that the interfacial strength is greater than the particle strength. Few cracks are observed in the Al matrix surface, as indicated by the yellow-colored dotted circle in Figure 4d. Also, the matrix cracks at the Al–SiC interface (yellow color arrow) during the transfer of tensile load from Al to SiC particles. Generally, preferred void nucleation via particle breakage and decohesion between the matrix and the reinforcement are lacking in fracture surfaces, as shown in Figure 4d–f. An excellent wetting between Al–SiC can be observed in Figure 4e,f for 6061/SiC and 7050/SiC MMCs, respectively. The SiC particles crack (white color arrow) when the local stress exceeds the particle fracture strength, which is characteristic of a strong particle–matrix bond. This is further evidence of strong interfacial bonding between Al and SiC in AMCs manufactured via the NISFAC process. These results were also confirmed via TEM observation at the SiC–matrix interface. As shown in Figure 5, the Al matrix is in very close contact with the SiC particle surface and there are no reaction products such as Al_4C_3 , which impairs the mechanical properties of the composite. This is probably because the NISFAC process has a much lower manufacturing temperature than the existing liquid-phase process (stirring and infiltration), suppressing the unwanted reaction products. The high-angle annular dark-field (HAADF) and high-resolution TEM (HRTEM) images are in Figure 5a and Figure 5b, respectively, exhibiting the Al–SiC interface structure in detail. The energy dispersive spectroscopy (EDS) mapping (Figure 5a) and fast Fourier transform (FFT) analysis (Figure 5b) at the interface of Al and SiC revealed a reaction layer and it was AlN . This reaction layer was formed due to the nitridation that occurred during the manufacturing of the composite material in a nitrogen atmosphere, which is consistent with the results of previous studies [32,33]. In addition, this reaction layer is very densely bonded at the atomic scale to the Al matrix and the SiC particles. The interfacial structure of composites is an essential factor affecting the overall properties

of composites. In particular, the mechanical properties of composites are determined via the interfacial strength between the reinforcement and the matrix, and the interfacial strength is determined via the physical and chemical interactions occurring at the interface. Therefore, good wetting is essential to create a robust interface. However, the binding force due to physical interaction is several kJ/mole in size, but the binding force due to chemical interaction is several hundred to several thousand kJ/mole [40]. Therefore, a limited reaction between the matrix and the reinforcing phase is required to form a strong interfacial bond. In addition, Drehmann et al. [41] deposited Al coatings on various ceramic substrates (Al_2O_3 , AlN, Si_3N_4 , and SiC) using a cold gas spraying process and then performed a tensile test to measure the adhesive strength. They found that the adhesion strength was not related to the difference in ionicity or CTE of the ceramic substrate and reported that the order of contact strength was $\text{AlN} > \text{SiC} > \text{Al}_2\text{O}_3 > \text{Si}_3\text{N}_4$. It was suggested that local heteroepitaxy between fcc-Al and w-AlN is a crucial factor facilitating adhesion as Al/AlN adhesion strength is the greatest.

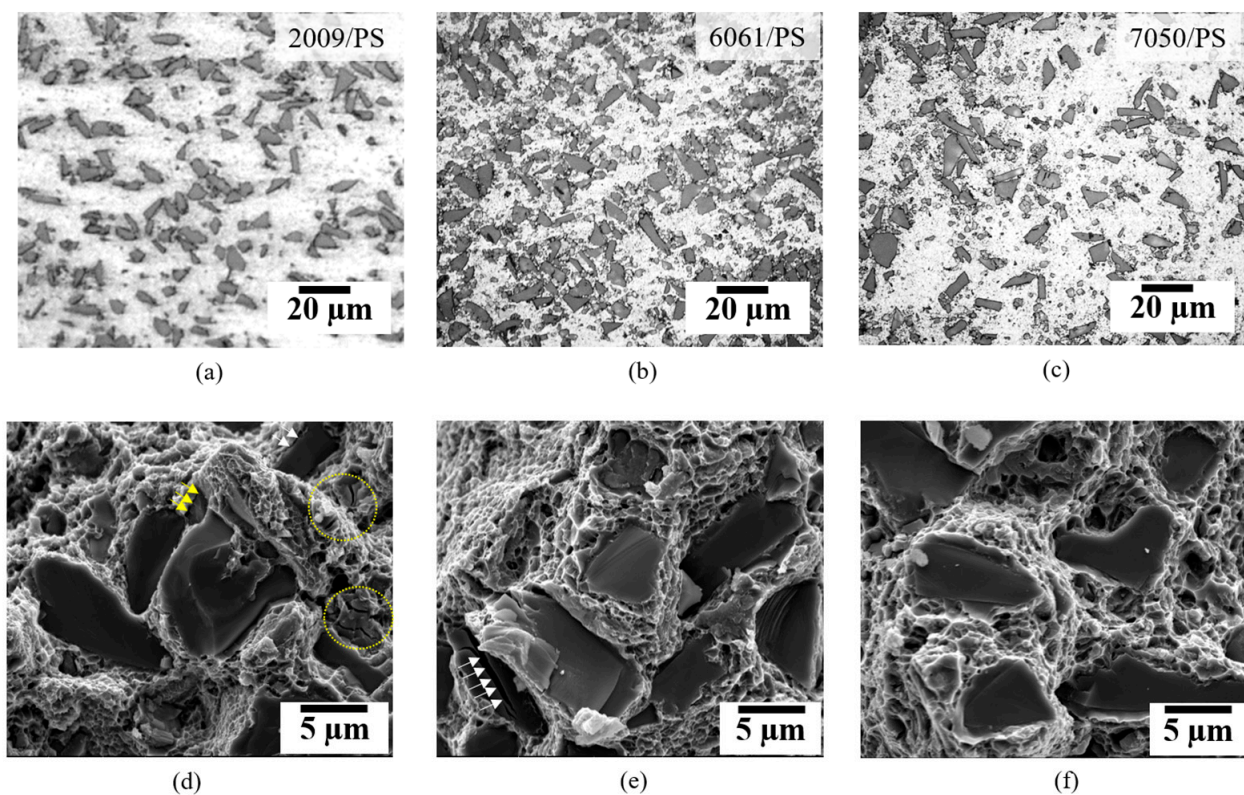


Figure 4. Micrographs of different NISFAC composites: optical micrograph of (a) 2009/PS, (b) 6061/PS, and (c) 7050/PS and SEM images of the tensile fracture surface of (d) 2009/PS, (e) 6061/PS, and (f) 7050/PS.

Figure 6 is a TEM observation of the 6061 Al/SiC (6061/PS) composite, which shows that the Al matrix is in very intimate contact (Figure 6a,b) with the surface of the SiC particles and that a reaction layer with a thickness of several nm containing very fine crystallites exists at the interface between the two phases (Figure 6c,d). These reaction products were identified as MgO and AlN via EDS mapping (Figure 6c) and FFT analysis (Figure 6d). Therefore, the excellent mechanical properties of the composites prepared via the NISFAC process can be attributed to the good wettability and the formation of AlN due to the nitridation reaction. The nitridation degree of the composites prepared in this study is about 0.5–1.9% (Table 2). This means that about 0.8 to 3 vol.% of AlN was formed by itself in the process of manufacturing the composite. Therefore, the fine AlN formed via the nitridation reaction may contribute to the mechanical properties by increasing the volume fraction of the reinforcing phase. The interfacial structure shown in Figures 5 and 6 implies

that the wettability problem between Al and SiC has been solved even though no artificial manipulations (pressure, stirring, and catalyst addition such as Mg) were applied during the composite manufacturing. Furthermore, it is essential to have a stiff phase comparable to SiC at the interface to ensure that the particle can contribute more effectively to load transfer, resulting in a higher Young's Modulus in the AMCs [8]. In the present study, the AMCs produced using the NISFAC process have a stiff AlN interlayer between Al and SiC, as seen in Figures 5 and 6, which further contributed to the improvement of Young's modulus in AMCs than their matrix.

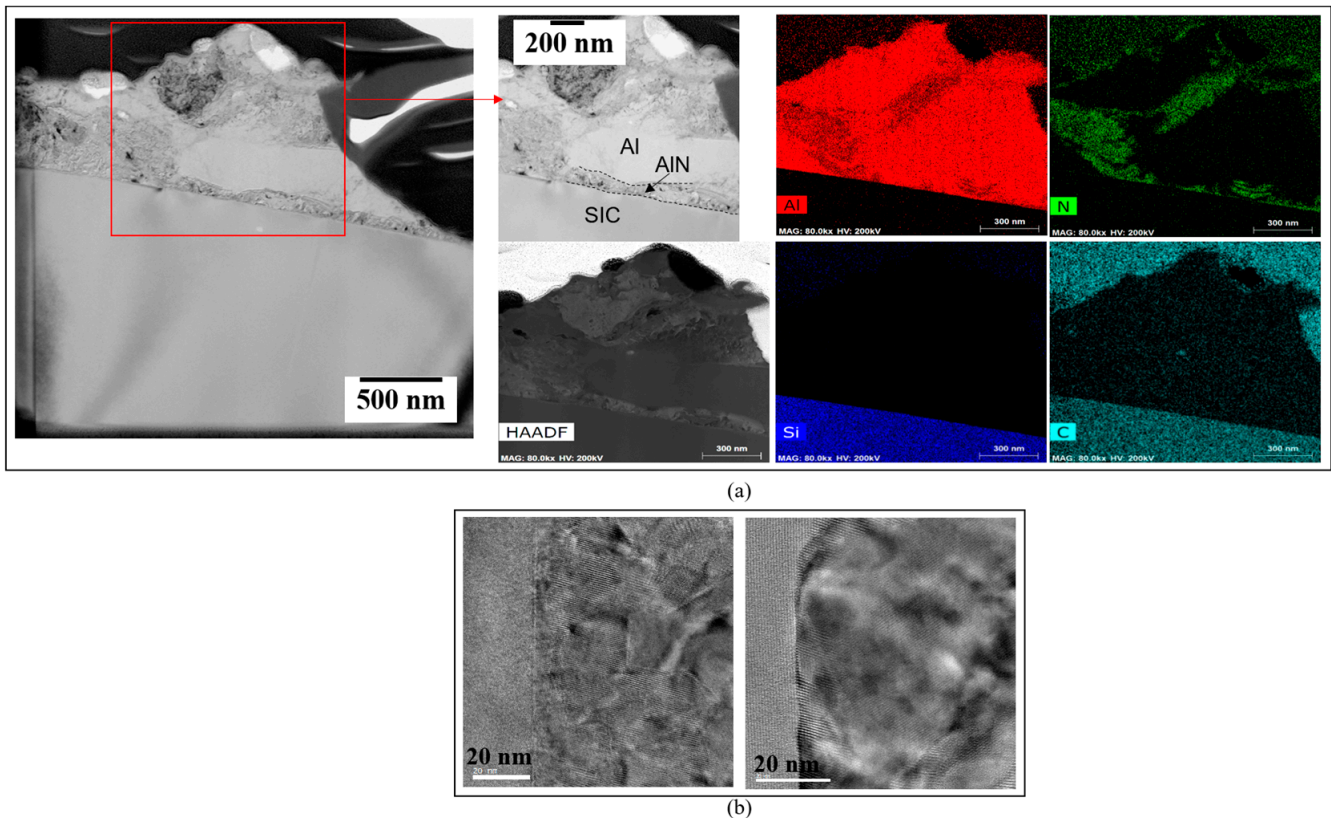


Figure 5. TEM images at matrix-SiC interface; (a) high-angle annular dark-field (HAADF) image and (b) high-resolution TEM (HRTEM).

The most significant advantage of the NISFAC process is that composites can be manufactured regardless of wettability. In other words, since there is no restriction on the type, size, and volume fraction of the reinforcing phase in the NISFAC process, it is possible to manufacture hybrid AMCs with various types of reinforcing phases added to the metal matrix, which can be tailored to the desired properties via the characteristics of the final product. This can be attributed to expanding product diversity and application fields. We continue to establish process conditions that exhibit optimal properties under various combinations of manufacturing conditions (type and size of Al and reinforcement phase, volume fraction, Al composition, manufacturing temperature, time, and nitrogen concentration) obtained through years of research. The presented results are the first results obtained from these studies. Therefore, it is believed that it will be possible to manufacture a composite material with improved properties if an optimal process is established.

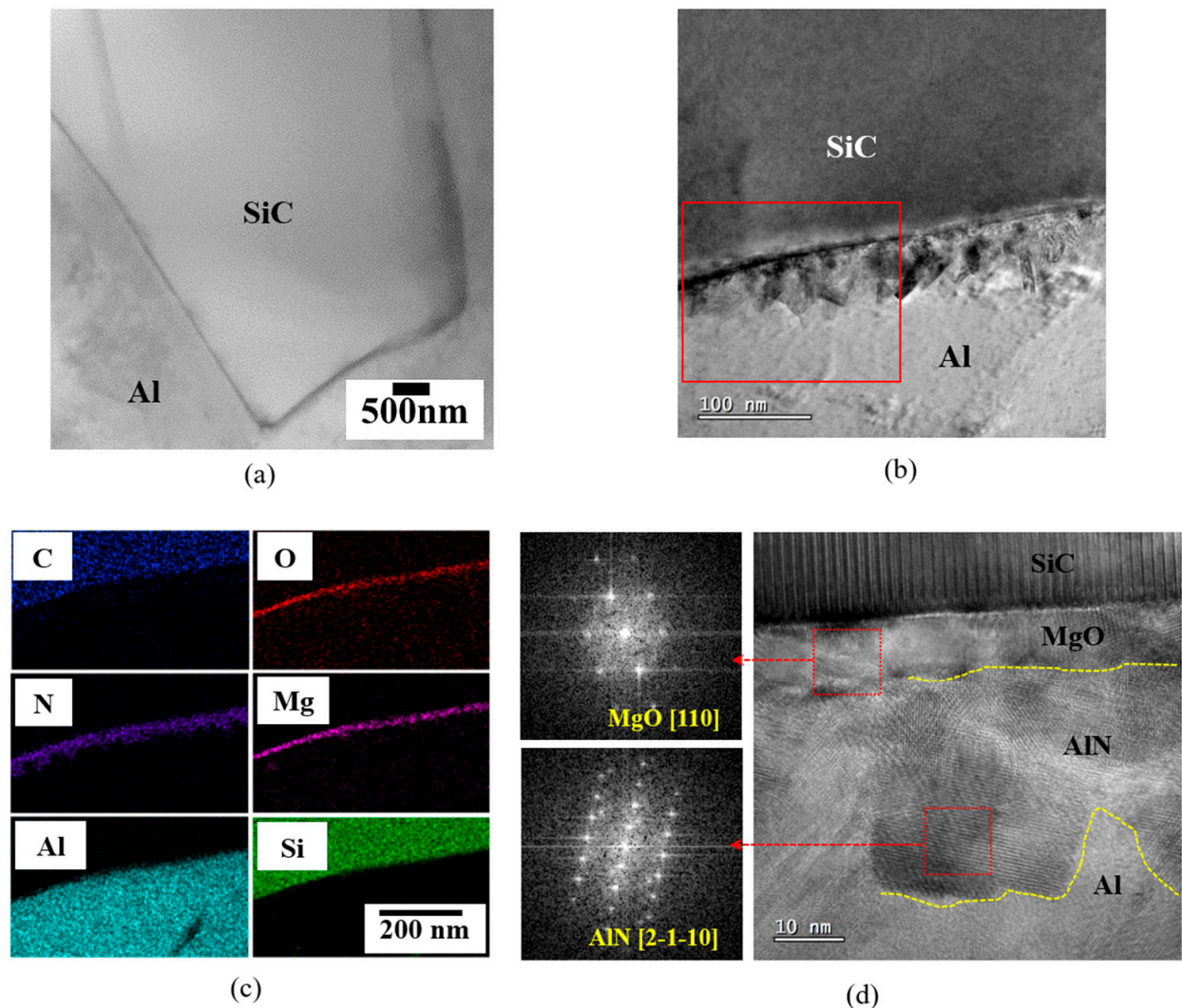


Figure 6. TEM micrographs at Al/SiC interface of 6061 Al/SiC (6061/PS); (a) TEM image showing Al and SiC, (b) magnified image at Al-SiC interface, (c) EDS mapping at Al-SiC interface in the red box on (b) at Al-SiC interface, and (d) HRTEM at Al-SiC interface with FFT at dashed red color box on (d).

4. Conclusions

This study compared the tensile properties of monolithic 6xxx alloys and 6xxx alloy matrix composites produced using the NISFAC process with those produced by representative commercial P/M companies. The results showed that the AMCs produced in this study had excellent tensile properties. In the case of the 6061 Al matrix, Young's modulus, yield strength, and ultimate tensile strength were increased by 59%, 66%, and 81%, respectively, compared to commercial monolithic 6061 alloys. Overall, the tensile properties of the composite manufactured via the NISFAC process were similar to or superior to those obtained in the existing commercial P/M process and it holds the potential for various applications in aerospace, defense, and the automotive sector.

Author Contributions: Conceptualization, K.-B.L.; Methodology, K.-B.L.; formal analysis, K.-B.L., K.C.N., C.-H.S. and J.-P.A.; investigation, K.-B.L., K.C.N., C.-H.S. and J.-P.A.; data curation, K.-B.L., K.C.N., H.-I.L. and S.-H.K.; extrusion and tensile test, H.-I.L. and S.-H.K.; TEM analysis, C.-H.S. and J.-P.A.; writing—original draft preparation, K.-B.L.; writing—review and editing, K.-B.L., K.C.N., H.-J.C. and J.-P.A.; supervision, H.-J.C.; project administration, K.-B.L. and H.-J.C.; funding acquisition, K.-B.L. and H.-J.C. All authors have read and agreed to the published version of the manuscript.

Funding: This research was supported by the National Research Foundation of Korea (NRF) grant funded by the Korea government (NRF-2021M3H4A1A04092462, NRF-RS-2023-00240406).

Data Availability Statement: All data included in the manuscript. No separate data are available for this manuscript.

Acknowledgments: The authors are grateful for funding from the National Research Foundation of Korea (NRF) grant funded by the Korea government (NRF-2021M3H4A1A04092462, NRF-RS-2023-00240406).

Conflicts of Interest: The authors declare no conflict of interest.

Appendix A

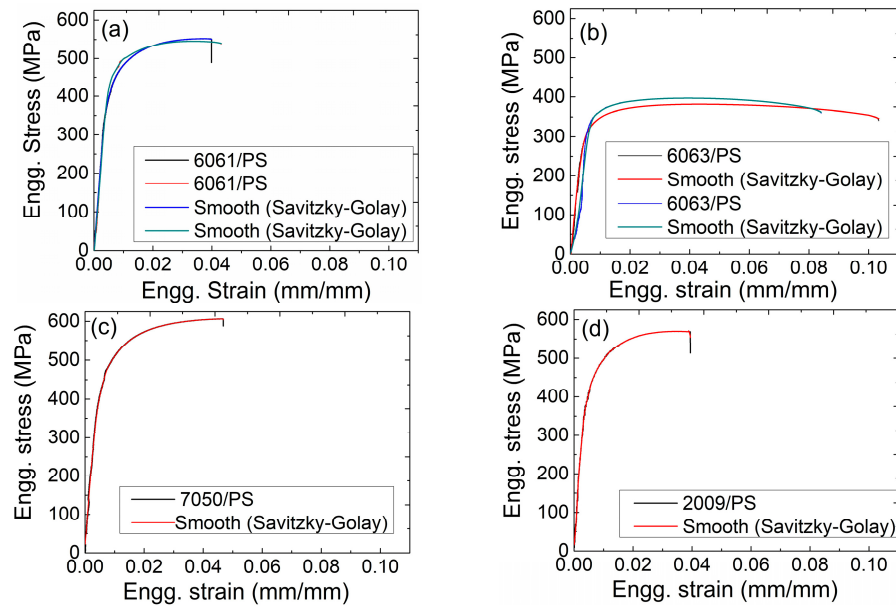


Figure A1. Representative stress–strain curves of different NISFAC-based AMCs; (a) 6061/PS, (b) 6063/PS, (c) 7050/PS and (d) 2009/PS.

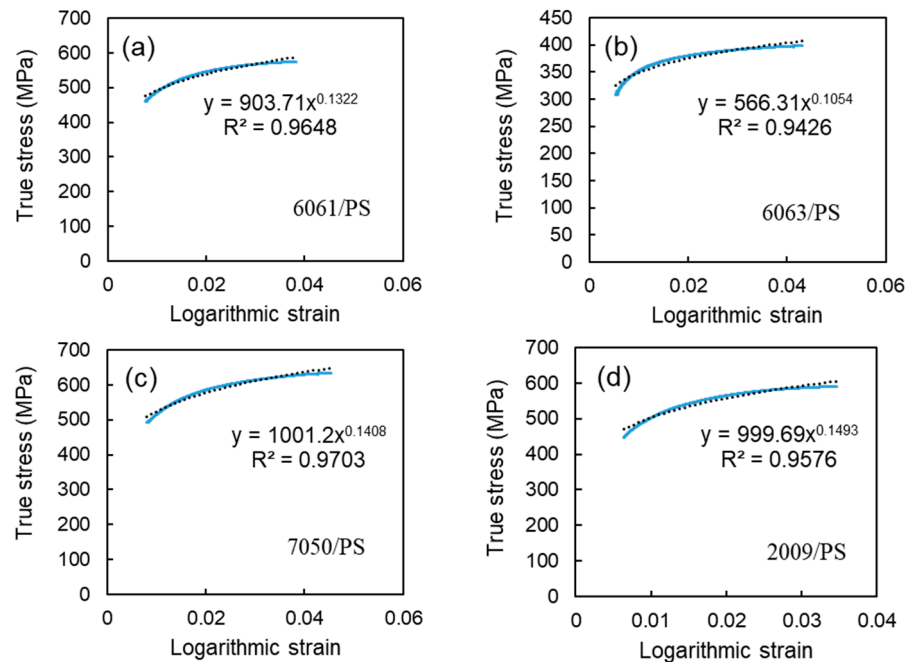


Figure A2. Flow stress behavior of different NISFAC-based AMCs; (a) 6061/PS, (b) 6063/PS, (c) 7050/PS and (d) 2009/PS.

References

1. Hooker, J.A.; Doorbar, P.J. Metal matrix composites for aeroengines. *Mater. Sci. Technol.* **2000**, *16*, 725–731. [CrossRef]
2. Samal, P.; Vundavilli, P.R.; Meher, A.; Mahapatra, M.M. Recent progress in aluminum metal matrix composites: A review on processing, mechanical and wear properties. *J. Manuf. Process.* **2020**, *59*, 131–152. [CrossRef]
3. Prasad, S.V.; Asthana, R. Aluminum metal-matrix composites for automotive applications: Tribological considerations. *Tribol. Lett.* **2004**, *17*, 445–453. [CrossRef]
4. Kaczmar, J.W.; Pietrzak, K.; Wlosinski, W. The production and application of metal matrix composite materials. *J. Mater. Process. Technol.* **2000**, *106*, 58–67. [CrossRef]
5. Wazeer, A.; Das, A.; Abeykoon, C.; Sinha, A.; Karmakar, A. Composites for electric vehicles and automotive sector: A review. *Green Energy Intell. Transp.* **2023**, *2*, 100043. [CrossRef]
6. Newswire, G. Metal Matrix Composite Market Size, Share & Trends Analysis Report by End-Use (Ground Transportation, Electronics), by Product (Refractory, Aluminum), by Region, and Segment Forecasts, 2020–2027. 2020. Available online: <https://www.grandviewresearch.com/industry-analysis/metal-matrix-composites-mmc-market> (accessed on 28 October 2023).
7. Parveez, B.; Kittur, M.I.; Badruddin, I.A.; Kamangar, S.; Hussien, M.; Umarfarooq, M.A. Scientific Advancements in Composite Materials for Aircraft Applications: A Review. *Polymers* **2022**, *14*, 5007. [CrossRef]
8. Krizik, P.; Balog, M.; Matko, I.; Svec, P.; Cavojsky, M.; Simancik, F. The effect of a particle-matrix interface on the Young's modulus of Al-SiC composites. *J. Compos. Mater.* **2016**, *50*, 99–108. [CrossRef]
9. Chawla, N.; Shen, Y.-L. Mechanical Behavior of Particle Reinforced Metal Matrix Composites. *Adv. Eng. Mater.* **2001**, *3*, 357–370. [CrossRef]
10. Lee, K.B.; Kwon, H. Strength of Al-Zn-Mg-Cu matrix composite reinforced with SiC particles. *Metall. Mater. Trans. A Phys. Metall. Mater. Sci.* **2002**, *33*, 455–465. [CrossRef]
11. Lee, K.B.; Sim, H.S.; Cho, S.Y.; Kwon, H. Tensile properties of 5052 Al matrix composites reinforced with B4C particles. *Metall. Mater. Trans. A Phys. Metall. Mater. Sci.* **2001**, *32*, 2142–2147. [CrossRef]
12. Tran, T.Q.; Lee, J.K.Y.; Chinnappan, A.; Loc, N.U.; Tran, L.T.; Ji, D.; Jayathilaka, W.A.D.M.; Kumar, V.V. High-performance carbon fiber/gold/copper composite wire for lightweight electrical cables. *J. Mater. Sci. Technol.* **2020**, *42*, 46–53. [CrossRef]
13. Tran, T.Q.; Lee, J.K.Y.; Chinnappan, A.; Jayathilaka, W.A.D.M.; Ji, D.; Kumar, V.V.; Ramakrishna, S. Strong, lightweight, and highly conductive CNT/Au/Cu wires from sputtering and electroplating methods. *J. Mater. Sci. Technol.* **2020**, *40*, 99–106. [CrossRef]
14. Mortazavian, S.; Fatemi, A. Effects of fiber orientation and anisotropy on tensile strength and elastic modulus of short fiber reinforced polymer composites. *Compos. B* **2015**, *72*, 116–129. [CrossRef]
15. Ogasawara, T.; Ishida, Y.; Kasai, T. Mechanical properties of carbon fiber/fullerene-dispersed epoxy composites. *Compos. Sci. Technol.* **2009**, *69*, 2002–2007. [CrossRef]
16. Almeida Jr, J.H.S.; Angrizani, C.C.; Botelho, E.C.; Amico, S.C. Effect of fiber orientation on the shear behavior of glass fiber/epoxy composites. *Mater. Des.* **2015**, *65*, 789–795. [CrossRef]
17. Hsieh, C.T.; Ho, Y.C.; Wang, H.; Sugiyama, S.; Yanagimoto, J. Mechanical and tribological characterization of nanostructured graphene sheets/A6061 composites fabricated by induction sintering and hot extrusion. *Mater. Sci. Eng. A* **2020**, *786*, 138998. [CrossRef]
18. Karthik, M.; Honnaiah, C.; Prasad, S.L.A.; Srinath, M.S. A Study on Fatigue Characteristics of Al-SiC Metal Matrix Composites Processed Through Microwave Energy. *IOP Conf. Ser. Mater. Sci. Eng.* **2018**, *376*, 1–6. [CrossRef]
19. Bhoi, N.K.; Singh, H.; Pratap, S. Developments in the aluminum metal matrix composites reinforced by micro/nano particles—A review. *J. Compos. Mater.* **2020**, *54*, 813–833. [CrossRef]
20. Chawla, K.K. *Composite Materials: Science and Engineering*, 3rd ed.; Springer-Verlag: New York, NY, USA, 2012.
21. Lee, K.B.; Yoo, S.H.; Kim, Y.H.; Han, C.W.; Won, S.O.; Ahn, J.P.; Choi, H.J. A cost-effective route to produce Al/AlN composites with low coefficient of thermal expansion. *J. Compos. Mater.* **2017**, *51*, 2845–2851. [CrossRef]
22. Huber, T.; Degischer, H.P.; Lefranc, G.; Schmitt, T. Thermal expansion studies on aluminium-matrix composites with different reinforcement architecture of SiC particles. *Compos. Sci. Technol.* **2006**, *66*, 2206–2217. [CrossRef]
23. Qu, X.H.; Zhang, L.; Wu, M.; Ren, S.B. Review of metal matrix composites with high thermal conductivity for thermal management applications. *Prog. Nat. Sci. Mater. Int.* **2011**, *21*, 189–197. [CrossRef]
24. Miracle, D.B. Metal matrix composites—From science to technological significance. *Compos. Sci. Technol.* **2005**, *65*, 2526–2540. [CrossRef]
25. Zweben, C. Metal matrix composites for electronic packaging. *JOM J. Miner. Met. Mater. Soc.* **1992**, *44*, 15–23. [CrossRef]
26. Lee, H.S.; Jeon, K.Y.; Kim, H.Y.; Hong, S.H. Fabrication process and thermal properties of SiCp/Al metal matrix composites for electronic packaging applications. *J. Mater. Sci.* **2000**, *35*, 6231–6236. [CrossRef]
27. Degischer, H.P.; Prader, P.; Marchi, C.S. Assessment of Metal Matrix Composites for Innovations—Intermediate report of a European Thematic Network. *Compos. Part A Appl. Sci. Manuf.* **2001**, *32*, 1161–1166. [CrossRef]
28. Idrisi, A.H.; Mourad, A.H.I. Conventional stir casting versus ultrasonic assisted stir casting process: Mechanical and physical characteristics of AMCs. *J. Alloys Compd.* **2019**, *805*, 502–508. [CrossRef]
29. Jung, J.; Kang, S. Advances in manufacturing boron carbide-aluminum composites. *J. Am. Ceram. Soc.* **2004**, *87*, 47–54. [CrossRef]
30. Rofman, O.V.; Prosviryakov, A.S.; Kotov, A.D.; Bazlov, A.I.; Milovich, P.O.; Karunakaran, G.; Mikhaylovskaya, A.V. Fabrication of AA2024/SiCp Metal Matrix Composite by Mechanical Alloying. *Met. Mater. Int.* **2022**, *28*, 811–822. [CrossRef]

31. Rosso, M. Ceramic and metal matrix composites: Routes and properties. *J. Mater. Process. Technol.* **2006**, *175*, 364–375. [CrossRef]
32. Lee, K.B.; Kim, S.H.; Kim, D.Y.; Cha, P.R.; Kim, H.S.; Choi, H.J.; Ahn, J.P. Aluminum matrix composites manufactured using Nitridation-Induced Self-Forming process. *Sci. Rep.* **2019**, *9*, 20389. [CrossRef]
33. Jang, H.; Kim, S.H.; Lee, N.; Cha, P.R.; Ahn, J.P.; Choi, H.J.; Lee, K.B. Mechanism for self-formation of Al matrix composites using nitridation-induced manufacturing processes. *J. Mater. Res. Technol.* **2022**, *18*, 2331–2342. [CrossRef]
34. Kim, D.Y.; Cha, P.R.; Nam, H.S.; Choi, H.J.; Lee, K.B. Effect of Material and Process Variables on Characteristics of Nitridation-Induced Self-Formed Aluminum Matrix Composites—Part 1: Effect of Reinforcement Volume Fraction, Size, and Processing Temperatures. *Materials* **2020**, *13*, 1309. [CrossRef] [PubMed]
35. DWA Aluminum Composites. 2005. Available online: <http://www.dwa-usa.com> (accessed on 28 October 2023).
36. Materion. 2005. Available online: <http://materion.com/products/metal-matrix-composites> (accessed on 28 October 2023).
37. Xu, W.; Li, Z.; Sun, X. Effect of Welding Speed on Mechanical Properties and the Strain-Hardening Behavior of Friction Stir Welded 7075 Aluminum Alloy Joints. *J. Mater. Eng. Perform.* **2017**, *26*, 1938–1946. [CrossRef]
38. Abood, A.N.; Saleh, A.H.; Abdullah, Z.W. Effect of Heat Treatment on Strain Life of Aluminum Alloy AA 6061. *J. Mater. Sci. Res.* **2013**, *2*, 51–59. [CrossRef]
39. Kalpakjian, S.; Schmid, S. *Manufacturing Engineering and Technology*, 2nd ed.; Prentice Hall: Wilmington, DE, USA; Pearson Education: Singapore, 2014; p. 62.
40. Rosazza, P.G.; Baffie, T.; Jeymond, M.; Eustathopoulos, N. Contact angles and spreading kinetics of Al and Al-Cu alloys on sintered AlN. *Mater. Sci. Eng. A* **2001**, *298*, 34–43. [CrossRef]
41. Drehmann, R.; Grund, T.; Lampke, T.; Wielage, B.; Wüstefeld, C.; Motylenko, M.; Schreiber, G.; Rafaja, D. Investigation of the bonding mechanisms of Al coatings on ceramic substrates deposited by cold gas spraying and magnetron sputtering. In Proceedings of the International Thermal Spray Conference, Long Beach, CA, USA, 11–14 May 2015; pp. 544–552. [CrossRef]

Disclaimer/Publisher’s Note: The statements, opinions and data contained in all publications are solely those of the individual author(s) and contributor(s) and not of MDPI and/or the editor(s). MDPI and/or the editor(s) disclaim responsibility for any injury to people or property resulting from any ideas, methods, instructions or products referred to in the content.